

to the marked concentration dependence, the peaks appearing in the 820-960 cm^{-1} region may be differentiated into three different kinds of species, namely $\text{Na}_x(\text{C}_6\text{H}_6)_y$, with $x > y$ (species 1), $x = y$ (species 2), and $x < y$ (species 3). One could assume that the peak being intensified along with the increase of sodium concentration, at a certain benzene concentration, is due to 'species 1'. Based on this, the 927 cm^{-1} peak could be attributed to 'species 1'. The relative invariance of the 927 cm^{-1} peak in the spectra of Figure 1(c) and (d) may be rationalized by assuming that the increase of sodium at higher benzene concentration does not affect greatly the amount of 'species 1'. On the other hand, one could assume that the peak being intensified at higher benzene concentration is due to 'species 3'. Based on this, the peaks appearing around 847, 895, and 914 cm^{-1} could be attributed to 'species 3'. Then, the peaks relatively insensitive to the concentration change, such as those around 855-859 cm^{-1} could be rendered to 'species 2'. Invoking further to the assignments made on the Li-C₆H₆ complexes,¹ it seems possible to render the peaks at 927, 914, and 859 cm^{-1} to $\text{Na}_2(\text{C}_6\text{H}_6)$, $\text{Na}(\text{C}_6\text{H}_6)_2$, and $\text{Na}(\text{C}_6\text{H}_6)$, respectively. Although the doublet at 855 and 859 cm^{-1} may be assigned together to 1:1 complex, the fact that the 855 cm^{-1} peak becomes more prominent in the annealed spectra, taken at higher sodium concentration (Figure 2(b) and (d)), suggests that the peak is more likely to arise from a 1:1 complex with 'x' being greater than 2 in $\text{Na}_x(\text{C}_6\text{H}_6)_y$. Assuming that the peaks at 847 and 895 cm^{-1} are together due to $\text{Na}(\text{C}_6\text{H}_6)_2$, the value of 'y' corresponding to the latter peak may be greater than that of the former since the latter appears distinctly only at a higher benzene concentration (Figure 1(c) and (d)). In addition, referring once again to the work on the Li-C₆H₆ complexes,¹ the peaks appearing in Figure 1 and 2 seem to be related with the ring breathing modes of appropriate complex species.

It would be worth to mention that even for the 1:1 Li-C₆H₆ complex, controversial views remain still on the nature of its structure. From an ESR study, Manceron *et al.*⁸ claimed the complex to assume a C_{2v} structure. This is in contrast with the approximation made earlier by Manceron and Andrews.¹ Benzene radical was, on the other hand, predicted to possess a D_{2h} symmetry based on the ab initio molecular orbital calculation.⁹ In order to resolve above controversy, information on other systems like Na-benzene will be much helpful.

In summary, it has been shown from the matrix isolation infrared spectroscopy that sodium atoms could form complexes with benzene, in contrast with the earlier work. Although the nature of complex species is not certain at the moment, a tentative assignment has been proposed. Further studies are required to characterize the identities of complex species. Accordingly, research is on progress to examine the isotope effect along with ab initio quantum mechanical calculation.

Acknowledgement. This work was supported by the S. N. U. Daewoo Research Fund, 1993 and by the Korea Science and Engineering Foundation (92-25-00-06). We acknowledge also the Ministry of Education, Republic of Korea, for its partial support to purchase instruments as a basic research program.

References

1. Manceron, L.; Andrews, L. *J. Am. Chem. Soc.* **1968**, *110*, 3840.
2. McCullough, J. D.; Duley, W. W. *Chem. Phys. Lett.* **1972**, *15*, 240.
3. Moore, J. C.; Thornton, C.; Collierm, W. B.; Delvin, J. P. *J. Phys. Chem.* **1981**, *85*, 350.
4. Kunze, K. R.; Hauge, R. H.; Hamitt, D.; Margrave, J. L. *J. Chem. Soc. Dalton Trans.* **1978**, 433.
5. Kim, H. S.; Kim, K. *Bull. Kor. Chem. Soc.* **1992**, *13*, 520.
6. Brown, K. G.; Person, W. B. *Spectrochim. Acta.* **1978**, *34A*, 117.
7. Andrews, L.; Johnson, G. L.; Davis, S. R. *J. Phys. Chem.* **1985**, *89*, 1706.
8. Manceron, L.; Schrimpf, A.; Bornemann, T.; Rosendahl, R.; Faller, F.; Stöckmann, H.-J. *Chem. Phys.* **1993**, *169*, 219.
9. Hinde, A. L.; Poppinger, D.; Radom, L. *J. Am. Chem. Soc.* **1978**, *100*, 4681.

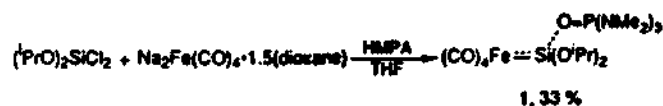
Synthesis, Characterization and Stability of $(\text{PrO})_2\text{Si}=\text{Fe}(\text{CO})_4 \cdot \text{HMPA}$

Myong Euy Lee, Joon Soo Han, and Chang Hwan Kim*

Department of Chemistry, Yonsei University,
Seoul 120-749

Received January 27, 1994

Recently, it has been demonstrated that silylene-transition metal complexes are stable as weak donor adducts.¹ Only ten examples of base-stabilized silylene complexes characterized by X-ray diffraction have been reported, and in all cases, coordination of a donor molecule to silicon is observed.¹² But little quantitative information on the stability and stereochemistry of these complexes has been published. We report here the synthesis and the characterization of a new donor-stabilized silylene complex, tetracarbonyl(diiisopropoxysilane)iron(0)-hexamethylphosphoramide, and the first experimental determination of the free energy of activation for losing stereochemistry at silicon of the donor-stabilized silylene complex.



The complex was synthesized by employing Collman's reagent, $\text{Na}_2\text{Fe}(\text{CO})_4$, as a metal source in reaction with dichlorodiiisopropoxysilane.^{10(a)-5} After recrystallization from diethylether, the compound **1** was obtained as a colorless crystalline complex.⁶ It melted at 139-140°C in a sealed capillary without decomposition. The presence of three carbonyl stretching bands (2007, 1926, 1888 cm^{-1}) indicates that the $\text{Fe}(\text{CO})_4$ moiety has the local C_{3v} symmetry and the silylene ligand occupies an apical position of trigonal bipyramid config-

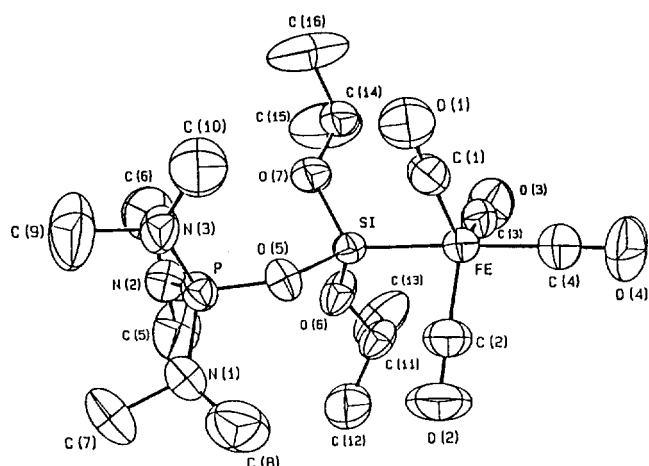


Figure 1. ORTEP view of $(t\text{PrO})_2\text{Si}=\text{Fe}(\text{CO})_4 \cdot \text{HMPA}$.

Table 1. Crystal Data, Data Collection, and Refinement of the Structure for 1

Formula	$\text{FePSiO}_7\text{N}_3\text{C}_{16}\text{H}_{32}$
fw	493.36
Space group	$\text{P2}_1/\text{n}$
a , Å	10.192(2)
b , Å	14.780(3)
c , Å	17.095(3)
β , deg	98.44(1)
V , Å ³	2547.4(8)
Z	4
d_{calc} , gcm ⁻³	1.286
Crystal size, mm	0.26 × 0.26 × 0.34
μ , cm ⁻¹	1.52
Scan method	w/2 θ
Data collected	$h, k, \pm 1, 3 < 2\theta < 44$
No. total observation	4948
No. unique data $> 3\sigma(I)$	2382
No. parameters refined	294
Abs. corr. factor range	0.966-0.999
gof	1.327
$R = (\sum F_o - F_c) / \sum F_o $	0.0494
$R_w = (\sum F_o - F_c W^{1/2}) / \sum F_o W^{1/2}$	0.0509

$$W = 1.3013/(\sigma^2(F) + 0.001314 F^2)$$

Table 2. Bond Distances (Å) and Bond Angles (deg) for 1

Fe-Si	2.261(2)	O(3)-C(3)	1.150(7)
Fe-C(1)	1.767(7)	O(4)-C(4)	1.143(7)
Fe-C(2)	1.748(6)	O(6)-C(11)	1.428(6)
Fe-C(3)	1.757(7)	O(7)-C(14)	1.410(7)
Fe-C(4)	1.778(7)	N(1)-C(7)	1.482(8)
P-O(5)	1.529(4)	N(1)-C(8)	1.444(9)
P-N(1)	1.611(5)	N(2)-C(5)	1.473(8)
P-N(2)	1.605(5)	N(2)-C(6)	1.473(9)
P-N(3)	1.606(5)	N(3)-C(9)	1.479(8)
Si-O(5)	1.711(3)	N(3)-C(10)	1.419(8)
Si-O(6)	1.618(4)	C(11)-C(12)	1.506(9)
Si-O(7)	1.633(4)	C(11)-C(13)	1.477(9)
O(1)-C(1)	1.149(7)	C(14)-C(15)	1.482(10)
O(2)-C(2)	1.153(7)	C(14)-C(16)	1.494(10)
C(1)-Fe-Si	86.3(2)	Si-O(5)-P	140.3(3)
C(2)-Fe-Si	85.0(2)	C(11)-O(6)-Si	132.5(4)
C(2)-Fe-C(1)	118.8(3)	C(14)-O(7)-Si	128.1(4)
C(3)-Fe-Si	83.4(2)	C(7)-N(1)-P	122.2(6)
C(3)-Fe-C(1)	117.6(3)	C(8)-N(1)-P	122.9(5)
C(3)-Fe-C(2)	121.3(3)	C(8)-N(1)-C(7)	113.1(7)
C(4)-Fe-Si	176.5(2)	C(5)-N(2)-P	121.6(6)
C(4)-Fe-C(1)	97.1(3)	C(6)-N(2)-P	122.0(5)
C(4)-Fe-C(2)	93.6(3)	C(6)-N(2)-C(5)	112.1(7)
C(4)-Fe-C(3)	94.6(3)	C(9)-N(3)-P	121.3(5)
N(1)-P-O(5)	105.3(2)	C(10)-N(1)-P	126.4(5)
N(2)-P-O(5)	117.9(2)	C(10)-N(2)-C(9)	112.2(6)
N(2)-P-N(1)	105.6(3)	O(1)-C(1)-Fe	178.9(5)
N(3)-P-O(5)	105.8(2)	O(2)-C(2)-Fe	179.2(6)
N(3)-P-N(1)	115.0(3)	O(3)-C(3)-Fe	178.6(6)
N(3)-P-N(2)	107.5(3)	O(4)-C(4)-Fe	178.2(7)
O(5)-Si-Fe	112.0(1)	C(12)-C(11)-O(6)	110.2(6)
O(6)-Si-Fe	118.8(2)	C(13)-C(11)-O(6)	107.5(6)
O(6)-Si-O(5)	102.8(2)	C(13)-C(11)-C(12)	112.5(8)
O(7)-Si-Fe	118.5(2)	C(15)-C(14)-O(7)	110.7(7)
O(7)-Si-O(5)	96.5(2)	C(16)-C(14)-O(7)	108.0(7)
O(7)-Si-O(6)	105.0(2)	C(16)-C(14)-C(15)	109.5(7)

at 1.32 ppm. These results strongly suggest that two methyl groups in the isopropoxy group are diastereotopic because of pyramidal-configured silicon atom.

In order to garner more conclusive evidences for the geometry of 1, X-ray crystal structure was determined. In Figure 1, the silylene ligand occupies an apical position at the $\text{Fe}(\text{CO})_4$ trigonal bipyramid, and the silicon atom is further complexed by the oxygen atom of the HMPA molecule. The silicon atom has a distorted tetrahedral geometry with a short Fe-Si bond (2.261 Å) and a long Si-O(HMPA) bond (1.711 Å) as shown in Table 2.

A line-shape analysis of variable temperature ^1H -NMR (80 MHz) spectra of 1 in toluene- d_8 afforded the first experimental data of the free energy of activation for losing stereochemistry at silicon, k (97°C) = 0.63 s⁻¹ and ΔG^\ddagger = 22 kcal/mol. The losing stereochemistry might be ascribed to the cleavage of Si-O bond in the adduct. Two doublets were not collapsed up to 100°C although they closed up significantly. The coale-

urated iron atom. The ^{13}C -NMR shifts of the carbonyl groups at 218.07 (s, CO_q) and 221.02 ppm (s, CO_{ap}) with a 3 : 1 ratio of intensity are in agreement with the TBP geometry of the iron atom. Molecular orbital analysis of d^8 TBP complexes predicts that good pi-accepting ligands prefer the equatorial position. The ^{29}Si chemical shift of 1 was observed at 20.9 ppm as a doublet ($^2J_{\text{FeSi}} = 25.6$ Hz).^{8,10b} Chemical shifts of low-valent silicon atoms are usually observed at down field.¹ Interestingly, two different methyl signals of isopropoxy groups were observed in ^1H and ^{13}C -NMR spectra of 1. In the case of ^1H -NMR, methyl protons of isopropoxy groups were observed as double doublets at 1.32 and 1.37 ppm. Two methyl groups in an isopropoxy group would have different chemical environments because the heptad of isopropoxy methine protons were decoupled to quartet by irradiation of the doublet

science temperature was not obtained successfully because of thermal decomposition of **1** at above 100°C.

Acknowledgement. This work was financially supported by Korea Science and Engineering Foundation. We are grateful to Dr. Il Nam Jung for getting the single crystal structure and helpful discussion.

References

- (a) Zybilla, C.; Müller, G. *Angew. Chem., Int. Ed. Engl.* **1987**, *26*, 669; (b) Zybilla, C.; Müller, G. *Organometallics* **1988**, *7*, 1368; (c) Straus, D. A.; Tilley, T. D.; Rheingold, A. L. *J. Am. Chem. Soc.* **1987**, *109*, 5872; (d) Ueno, K.; Tobita, H.; Shimoi, M.; Ogino, H. *J. Am. Chem. Soc.* **1988**, *110*, 4092; (e) Strauss, D. A.; Zhang, C.; Quimbata, G. E.; Grumbine, S. D.; Heyn, R. H.; Tilley, T. D.; Rheingold, A. L.; Geib, S. J. *J. Am. Chem. Soc.* **1990**, *112*, 2673; (f) Zybilla, C. *Nachr. Chem. Tech. Lab.* **1989**, *37*, 248.
- (a) Woo, L. K.; Smith, D. A.; Young, V. G., Jr. *Organometallics* **1991**, *10*, 3977; (b) Takeuchi, T.; Tobita, H.; Ogino, H. *Organometallics* **1991**, *10*, 835 and references therein.
- (a) Zybilla, C.; Wilkinson, D. L.; Müller, G. *Angew. Chem., Int. Ed. Engl.* **1988**, *27*, 583; (b) Zybilla, C.; Wilkinson, D. L.; Leis, C.; Müller, G. *ibid.* **1989**, *28*, 203.
- (a) Stewart, R. P.; Hensley, D. W.; Wurster, W. L. *Organometallic Syntheses* **1988**, *4*, 134; (b) Finke, R. G.; Sorell, T. N. *Org. Syn.* **1979**, *59*, 102; (c) Collman, J. P.; Finke, R. G.; Cawse, J. N.; Brauman, J. I. *J. Am. Chem. Soc.* **1977**, *99*, 2515.
- Jirinec, S.; Bazant, V.; Chvalovsky, V. *Collection Czechoslov. Chem. Commun.* **1961**, *26*, 1815.
- Data: HRMS (70 eV EI, m/z) calcd. for C₁₆H₃₂FeN₃O₇PSi: 493.1088. Found: 493.1079. ¹H-NMR (δ): 1.32, 1.37 (dd, ³J = 6.0 Hz, Me₂CH, 6H), 2.20 (d, ³J_{PH} = 10.4 Hz, Me₂N, 9H), 4.85 (h, ³J = 6.0 Hz, Me₂CH, 2H). ¹³C[¹H]NMR (δ): 25.73 (s, Me₂CH), 25.74 (s, Me₂CH), 36.43 (d, ³J_{PC} = 6.0 Hz, Me₂N), 65.00 (s, Me₂CH), 218.07 (s, CO_{eq}), 221.02 (s, CO_{ap}). ²⁹Si[¹H]NMR (δ): 20.9 (d, ²J_{PSi} = 25.6 Hz). IR (cm⁻¹): 2007, 1926, 1888 (ν_{CO}, THF soln), 765 (ν_{PN}, KBr pellet).

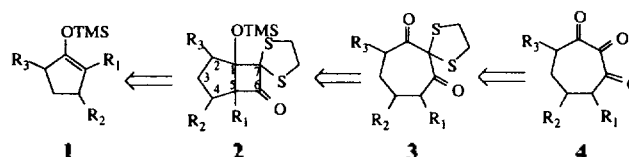
Ring Cleavage of Cycloadduct from [2+2] Thermal Cycloaddition of Dimethylene Dithioketene to Silyl Enol Ether

Chwang Siek Pak* and Sung Kee Kim

Korea Research Institute of Chemical Technology,
P.O. Box 107, Yousung, Taejon 305-606

Received January 27, 1994

Cycloadducts derive from [2+2] photoaddition¹ or thermal addition² have been utilized for the construction of various natural product skeletons.³ Fragmentation of the cycloadducts was usually performed by ionic and thermal reactions.⁴ Radical type fragmentation was also reported.⁵ Recently, we reported a ring expansion methodology to prepare



Scheme 1.

Table 1. Cycloaddition and Fragmentation Products from Silyl Enol Ether

Entry	Silyl enol ethers	Cycloadducts ^{a,b} (yield %)	Fragmentation products ^{c,d}
1			
2			
3			
4			
5		No Reaction	
6			
7		No Reaction	
8			

^aIsolated yields after column chromatography. ^bYields based on 2-chloro carbonyl thiolane. ^cDiketone is in equilibrium with enol forms (by ¹H-NMR). ^dIsolated yields without further purification are quantitative. (one spot on TLC).

substituted cycloheptenones *via* fragmentation of the corresponding 1-trimethylsilyloxy bicyclo [3.2.0] heptan-6-ones.⁶ In our continuing effort to expand the scope of this methodology, we have chosen dimethylene dithioketene for cycloaddition in order to develop a general route for triketo compounds **4** as described in Scheme 1.

In this communication, we report the unusual bond cleavage of silyl ethers **2** in the course of fluoride ion induced fragmentation. Fragmentation reactions of α -di- and trimethylenedithio group substituted cyclic ketones were previously reported.^{7,9,10} Bond cleavage of these precedents occurred consistently at C₆-C₇ by attack of a nucleophile due to the ring strain and anion stabilizing ability of sulfur atom. However, fragmentation of C₁-C₇ of compound type **2** were not found in the literature.